

A Novel Technique for Spatial Objects Shaping with a High-Pressure Abrasive Water Jet

Przemyslaw Borkowski

Institute of Unconventional HydroJetting Technology, Koszalin University of Technology, Poland

A novel method for the 3D shaping of different materials using a high-pressure abrasive water jet is presented in the paper. For steering the movement process of the jet a principle similar to the raster image way of record and readout was used. However, respective colors of pixel of such a bitmap are connected with adequate jet traverse speed that causes erosion of material with adequate depth. Thanks to that innovation, spatial imaging of the object can be observed. Theoretical basis as well as spatial model of material shaping and experimental stand including steering program are presented. Methodic and some experimental erosion results as well as practical examples of object's bas-relief made of meta are also presented.

©2010 Journal of Mechanical Engineering. All rights reserved.

Keywords: high-pressure abrasive water jet, material shaping

0 INTRODUCTION

The development of the high-pressure abrasive water jet (AWJ) machining method is mainly the result of tool elasticity and the fact that the technique never causes any structural changes in the substrate. Water jets were first used in the 1980s, and since then, much research has been done to optimize the technology and improve the cutting efficiency. An examination of the abrasive grain interaction in the treatment zone led to an understanding of the mechanism of abrasive erosion [1] to [6], making it simpler to characterize and execute milling processes [7]. Precision and quality of the treated surfaces were analyzed. Water jet techniques can be applied to brittle [8] and [9] and ductile materials such as aluminum and titanium alloys [9]. A number of experiments [10] and [11] have clarified the mechanisms of abrasive water jet cutting that define eroded grooves shape [12] and [13], process characteristics [14], as a prediction of cutting parameters [15] and [16]. This knowledge led to simulations of efficiency [17] and cost [16] and [18].

As a result of better understanding the cutting mechanism, techniques such as milling [7] and surface treatment [19] have become possible. Recently, a new method of automatic abrasive water jet sculpturing [20] and [21] of different materials was presented. It enables the production

of spatial shaping of an object based on a photograph [22] and [23].

In order to manipulate the position of the jet, a principle similar to image rastering was employed. Here, the color of a pixel in the image is correlated to a specific jet traverse speed that induces erosion of the substrate to a particular depth [22] and [24]. Owing to this innovation, spatial imaging of the object can be observed.

The concept of spatial material shaping depends on determining the light intensity on the surface of a target object from an image. In practice, this process controlled by a computer navigation program that reads the object's image and then steers the working heads and regulates their traverse speeds [21] and [22]. Its longitudinal movement is velocity-controlled by an analog input, which allows for continuous control of the degree of material removal caused by the abrasive water jet [20].

By referencing the pitting pattern left in the wake of the jet, it is possible to relate the depth of a given cut to the desired pattern in the target image [24]. The amount of time that the jet interacts with the substrate is proportional to the expected erosion depth, and this allows traverse speed to be used as the governing parameter for erosion depth. In this case, the smallest treatable area is determined by the diameter of the jet. The combination of different jet interactions with the substrate allows a spatial bas-relief of the real object to be constructed [23].

*Corr. Author's Address: Koszalin Univ. of Technology, Raclawicka 15-17, 75-620 Koszalin, Poland, przemyslawborkowski@wp.pl

1 THEORETICAL BASIS

The essence of this method consists of properly specifying the erosion depth and working head positions in relation to the minimum resolution required to capture the target feature. The method relies on image rastering to address each pixel and to construct the whole image. Owing to the similarity between this method and data manipulation of rastered images, the bitmap file format was used as the standard. For such bitmaps, respective pixel colors are correlated to specific erosion depths. The essence of this method is illustrated in Fig. 1.

The following steps are required for this technique:

1. The image, typically a photograph, is scanned in gray-scale.
2. The pixel values in the resulting bitmap are converted to working head traverse speeds that determine the jet interaction time at each location on the substrate.
3. The traverse speeds are passed to the water jets, and the image geometry is parsed into the control language of a 2-axis plotter that physically rasters the jets across the substrate.

While this approach requires only a simple 2-axis plotter, position control of the jets is crucial, and a specialized program to parse the image data in the control language of the plotter is required.

All actions related to process configuration are performed by the user according to a strict procedure [23]. Once prepared, the software records the settings and initializes the appropriate modules. Image processing can be performed by using a filter that transforms bitmaps into 256 step gray scale images based on calculating the luminance from an RGB image according to [21].

$$Grey\ depth = 0.3 \cdot Red + 0.59 \cdot Green + 0.11 \cdot Blue. \quad (1)$$

Intensity of illumination determines the quality of the resulting image from a photograph. Therefore, special care should be taken when creating the target images because the quality of these images relates directly to the quality of the product. A basic photometric quantity is luminance of a luminous surface in a given direction, which can be expressed as

$$L = \frac{\Delta I}{\Delta S \cos \varepsilon} = \frac{\Delta \Phi}{\Delta \omega \Delta S \cos \varepsilon}, \quad (2)$$

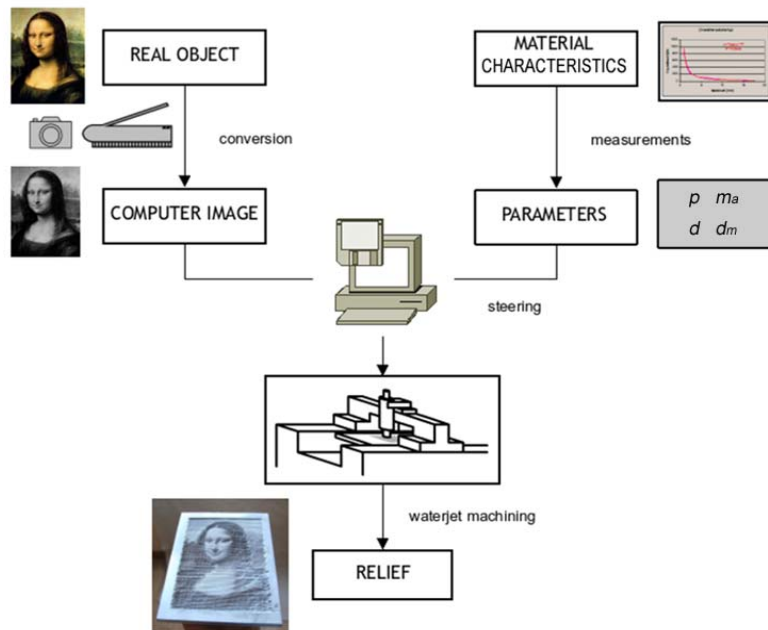


Fig. 1. 3D material forming with utilization of flat virtual object luminance

where: ΔI is light intensity, $\Delta\Phi$ is energy flux, ΔS is surface radiation, $\Delta\omega$ is a block angle relating object surface illumination to the light beam, while ε is the angle between the vector normal to the surface of ΔS and the direction of radiation propagation.

Differences in the surface morphology of the target object cause the ε angle and luminance of each element to have unique values. To a certain extent, the automated method of object quasi-spatial sculpturing based on a target image needs to evaluate the relation between photometric conditions of visible light radiation and jet erosion parameters. Therefore, both radiation and jet dynamics must be modeled.

Considering Eq. (2), where the energy flux ($\Delta\Phi = \frac{\Delta W}{\Delta t}$) defines light energy (ΔW) emitted in time (Δt), one can evaluate the proper exposure time for a given target object. This time value defines the interaction time of the water jet with respect to each elementary cell of the treated material that is approximately equal to the focusing nozzle diameter (d_m). This proportion can also be expressed via

$$\frac{K_m \Delta W}{L_i \Delta\omega \Delta S \cos \varepsilon_i} = \frac{d_m}{V_i}, \quad (3)$$

where K_m is a photometric equivalent of radiation, ΔW is emission energy, L_i is the luminance of a given element (i) taken from the target image, ε_i is the angle between the vector normal to the surface and the direction of radiation propagation while V_i is the velocity of the jet movement above the chosen elementary cell (i) of shaped material.

Imaging the target takes place using perpendicular radiation and perpendicular abrasive-water jet spraying ($\varepsilon = \varepsilon_i = 0^\circ$). Substituting these parameters into Eq. (3), one can evaluate the instantaneous velocity of the jet motion above a given element. This is described by the following equation:

$$V_i = A L_i, \quad (4)$$

where $A = \frac{\Delta\omega \Delta S d_m}{K_m \Delta W}$ is a constant involving photometric conditions and characteristics of the working head used for AWJ treatment.

Instead of attempting to model full dynamic process control, a simplified model [22] of the direct coupling between traverse speed (V) and erosion depth (h) was applied. It is expressed in the form of the following power equation:

$$h = b V^{-a}, \quad (5)$$

where a is the power exponent, and b is an empirical factor.

Based on this analysis, the depth of material erosion is proportional to a negative power function of jet traverse speed. This implies that the deepest erosion takes place at a minimum jet traverse speed, while increasing the traverse speed leads to reduced erosion according a nearly hyperbolic dependence. This relation is also suitable for instantaneous values of h_i , V_i related to erosion of a given element.

Substituting Eq. (4) into (5), a new formula to determine the instantaneous values of eroded material is obtained:

$$h_i = B L_i^{-a}, \quad (6)$$

where $B = b \left(\frac{\Delta W K_m}{\Delta\omega \Delta S d_m} \right)^a$ is a new factor involving photometrical and characteristics of the working head.

Examining this universal model Eq. (6) shows that material erosion depth is proportional to a negative power function of a given elements luminance. In the effect, the most shaded parts of an image correspond with the deepest material erosion, while an increase in luminance leads to a quasi-hyperbolic decrease in erosion depth.

Application of such a model simplifies the raster control method and increases treatment accuracy by enabling the erosion depth to be specified.

2 EXPERIMENTAL STAND

A special experimental stand was designed and built (see Fig. 2). Two stepper-driven lead screws (WX6 08500 by Isert Electronic) were used as linear actuators to control the planar position of the working head, while an additional lead screw system was affixed to these to provide a base for the working head. This gantry ensures XY positioning accuracy of ± 0.005 mm over a table area of 1000 x 1000 mm. This customized gantry supported a water supply to the working head that was pressurized up to 50 MPa, thereby ensuring constant traverse speed of the abrasive material from the reservoir. Longitudinal movements of the head were produced with stepping frequencies of 1 to 2400 s^{-1} that taking lead screw travel in account, gives a traverse

speed of approximately 0.005 to 12 mm/s, allowing a wide range of different cuts to be made.



Fig. 2. A general view of test stand for spatial material machining with high pressure abrasive-water jet: 1) frame, 2) y direction slideways, 3) x direction slideway, 4) abrasive-water jet working head, 5) abrasive feed container, 6) steering PC computer, 7) high-pressure water pump type As500/15A

The actual control of the water jet was controlled with a custom-made WaterJetLab software that was written in C++. The FreeDOS platform was used to provide access to PC hardware. This system handles all of the aforementioned functions in only 5000 lines of code, has easily obtainable hardware requirements and presents a simple user interface. Different ceramics, glasses, plastics and popular metals served as sample materials. Aluminum alloy, 5 mm thick AlMg1SiMn, was used most commonly. Depending on the shape of the object to be reproduced, the maximum erosion depth

defined in the WaterJetLab program was set to values ranging from 1.5 to 2.5 mm. A water nozzle of 0.7 mm diameter and focus nozzle of 2.5 mm diameter was installed in the work head, while a standoff distance was set at 5 mm. Experiments were conducted with a water pressure range of 10 to 50 MPa, while garnet #80 or #120 was used as the abrasive material and was set to output at 0.28 to 0.9 g/s.

3 EROSION CHARACTERISTICS OF MATERIALS

Calibration of the material's erosive properties was then conducted. The erosion characteristics of the jet are determined by the physical properties of substrate material. The optimal jet properties such as water pressure (p), abrasive material type and output (m_a), interaction time and the jet spraying angle (α) all depend on the substrate properties. Typical examples of this are seen in Fig. 3, which depicts the erosion of AlMg1SiMn under different test conditions. Specific equations describing parameter-specific metal erosion models are presented in Table 1.

4 BAS-RELIEF JETTING EFFECTS

Using this system and approach, basic metal shaping experiments were conducted. Two particular types of test were performed to characterize quality and accuracy and to assess the practicality of the technique.

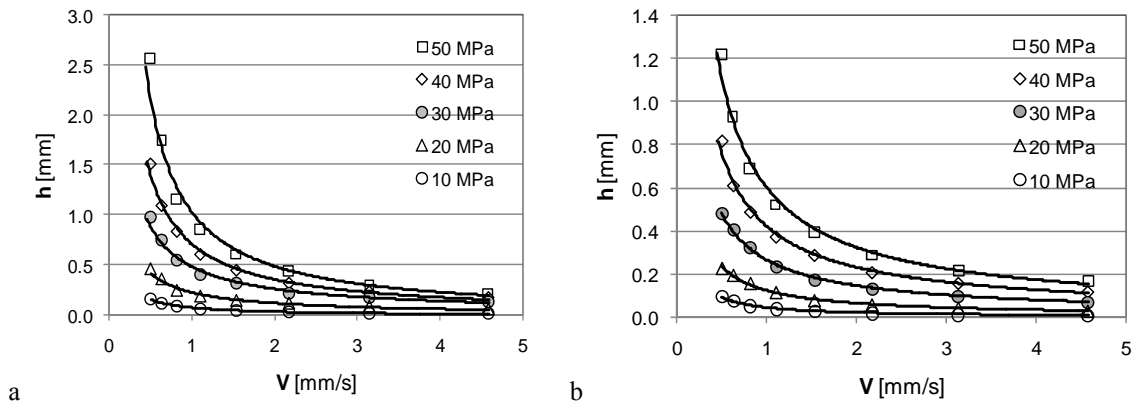


Fig. 3. AlMg1SiMn erosion realized with abrasive-water jet technology: a) garnet #120, $m_a = 0.90$ g/s, b) garnet #120, $m_a = 0.56$ g/s

Table 1. Models of aluminum alloy (AlMg1SiMn) erosion presented for different work condition (garnet #120)

| p [MPa] | m_a [g/s] | | |
|-----------|-----------------------|-----------------------|-----------------------|
| | 0.28 | 0.56 | 0.90 |
| 50 | $h = 0.352 V^{-0.76}$ | $h = 0.606 V^{-0.85}$ | $h = 1.037 V^{-1.01}$ |
| 40 | $h = 0.233 V^{-0.84}$ | $h = 0.425 V^{-0.83}$ | $h = 0.717 V^{-0.93}$ |
| 30 | $h = 0.145 V^{-0.83}$ | $h = 0.264 V^{-0.84}$ | $h = 0.485 V^{-0.88}$ |
| 20 | $h = 0.074 V^{-1.04}$ | $h = 0.125 V^{-0.91}$ | $h = 0.233 V^{-0.86}$ |
| 10 | $h = 0.023 V^{-0.87}$ | $h = 0.042 V^{-1.15}$ | $h = 0.077 V^{-0.99}$ |

Basing on this prototype jet-machine, a wide array of different uses for abrasive water jets were considered. This process needs neither complicated process control nor complex position control. Adequate software of such jet machining processes need only to ensure the possibility for proper “relocation” between sample material features and abrasive-water jet erosiveness and working head traverse speed that is finally responsible for material spatial sculpturing basing on the photo.

Examinations of the effect of material on the ability to produce a particular shape with a

high-pressure abrasive-water jet led to the collection of interesting data. Specifically, it was determined that erosion depth can be verified and that spatial objects can be produced based on flat image templates. Common results from such work can be seen in the following pictures.

Fig. 4 presents a photocopy of a well known painting and includes a set of illustrations showing the important phases of its reproduction in a metal plate. Obtained in this way, the final bas-relief represents relatively good quality thanks to fine quality of the initial image.

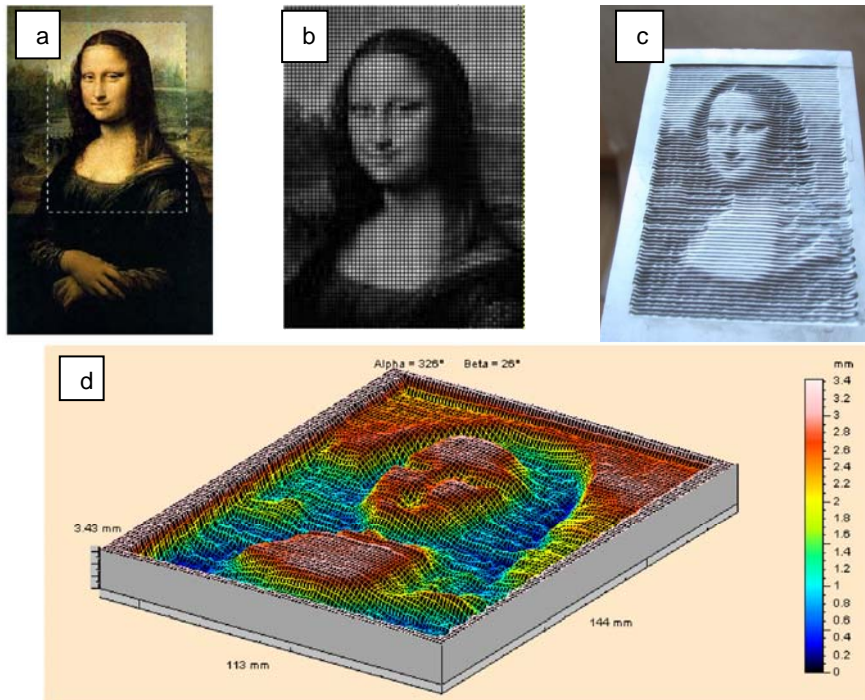


Fig. 4. Images showing important phases of spatial object (Mona Lisa) AWJ sculpturing ($p = 50$ MPa, garnet #80, $m_a = 0.90$ g/s) basing on its photocopy: a) picture, b) virtual 2D matrix, c) photo of 3D bas-relief cut in AlMg1SiMn plate, d) image scanned from the relief

While there is enormous advantage in the automated water jet cutting technique presented, inaccuracy was noted in the form of incomplete reproduction of the erosion depth in regions of high contrast compared to the surroundings [21]. It was observed that proper erosion depth can be achieved only when consecutive pixels in a rastered line share fairly similar gray scale values [22] and [23]. Moreover, the quality needs to be improved with respect to the boundary leveling that occurs between individual lines (Fig. 5).

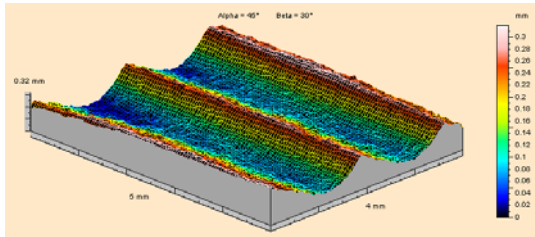


Fig. 5. Shape regularity and edge height of respective jet paths after AWJ treating of AlMg1SiMn for $p = 40 \text{ MPa}$, garnet #120, $m_a = 0.56 \text{ g/s}$

Surface quality shaped with AWJ jet depends on spray angle (Fig. 7) and its effect is similar to grinding because the resultant surface creates a mosaic of irregular traces created after abrasive grains stroke.

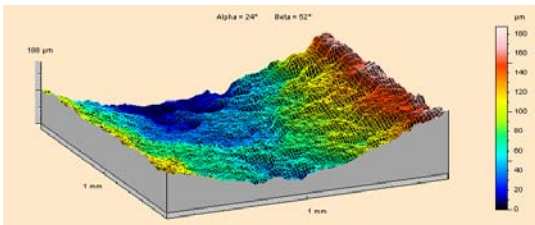


Fig. 6. Quality of the bottom of eroded region for AWJ treating of AlMg1SiMn ($p = 50 \text{ MPa}$, garnet #120, $m_a = 0.90 \text{ g/s}$)

Elimination of this problem is possible by modifying the algorithm determining positive and negative gradients with respect to the desired erosion depth. Previous measurements of the effects of such a correction demonstrate a marked improvement in quality [20] and [22]. One should bear in mind that during such abrasive water jet spraying, surface of the sample becomes slightly

tarnished based on the roughness parameters shown in Fig. 6.

It can be claimed that, despite the relatively low matrix resolution, the quality of the reproduced image in metal plates is satisfactory. Further, it should be noted that characteristics of the target object are preserved. A particular example of this may be seen in the still recognizable subtle smile of La Gioconda presented in Fig. 4. Despite the problem discussed earlier, these results suggest a good future for this technology.

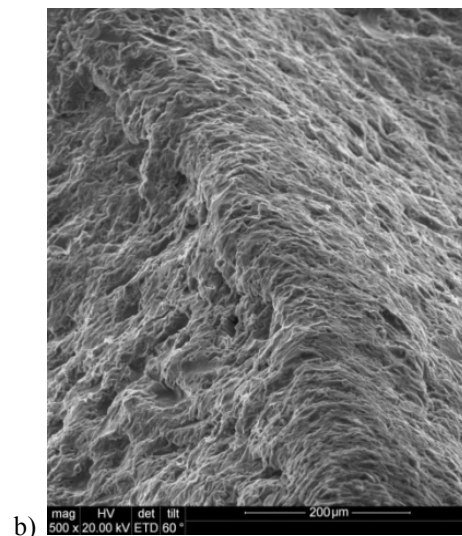
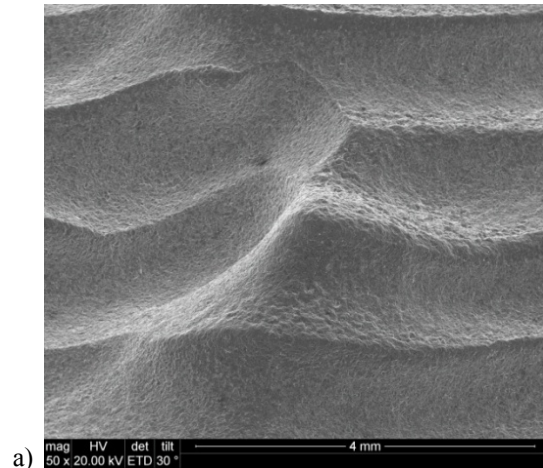


Fig. 7. Typical configuration of a) macro and b) micro surface eroded in aluminum alloy (AlMg1SiMn, $p = 40 \text{ MPa}$, garnet #120, $m_a = 0.56 \text{ g/s}$)

5 SUMMARY

The abrasive water jet based material shaping technique presented here confirms the assumptions about water jet machining and presents a software based procedure for controlling the position of the work head. Based on the presented data, it can generally be admitted that, despite the low matrix resolution, images given in the form of bitmaps were reconstructed relatively well in metal samples. Therefore, the presented method gives satisfactory results.

6 REFERENCES

- [1] Deam, R.T., Lemma, E., Ahmed, D.H. (2004). Modelling of abrasive water jet cutting process. *Wear* 257, p. 877-891.
- [2] Finnie, I. (1962). Erosion by solid particles in a fluid stream. *Erosion and Cavitation. ASTM STP*, 307, p. 70-82.
- [3] Lebar, A., Junkar, M. (2004). Simulation of abrasive water jet cutting process: Part 1. Unit event approach. *Modelling Simul. Mater. Sci. Eng.*, vol. 12, no. 6, p. 1159-1170.
- [4] Obranić, H., Junkar, M. (2004). Simulation of abrasive water jet cutting process: Part 1. Cellular automata approach. *Modelling Simul. Mater. Sci. Eng.*, vol. 12, no. 6, p. 1171-1184.
- [5] Obranić, H., Junkar, M. (2007). Analysis of striation formation mechanism in abrasive water jet cutting. *Wear*, 265 (5/6), p. 821-830.
- [6] Hashish, M. (1984). On the modeling of abrasive-waterjet cutting. *Proc. 7th Int. Symposium on Jet Cutting Technology*, Ottawa, Paper E1, p. 249-265.
- [7] Hashish, M. (1989). An investigation of milling with abrasive-waterjets. *Trans. ASME, Journal of Engineering for Industry*. vol. 111, no. 2, p. 158-166.
- [8] Lauand, V.H., Hennies, W.T., Stellin, A. Jr. (2008). Glass and marble (Cachoeiro de Itapemirim) milling with abrasive water jetting. *Proc. 19th Int. Conference Water Jetting*, BHR Group, Nottingham, p. 121-139.
- [9] Zhang, S., Galecki, G., Summers, D.A., Swallow, C. (2007). Use of pre-profiling a milled pocket as a means of improving machining and lowering energy costs. *Proc. 2007 WJTA Conference and Expo*, Houston, Paper 3-H.
- [10] Groppetti, R., Gutema, T., Di Lucchio, A. (1998). A contribution to the analysis of some kerf quality attributes for precision abrasive water jet cutting. *Proc. 14th Int. Conf. on Jetting Technology*, Brugge, p. 253-269.
- [11] Tan, D.K.M. (1986). A model for the surface finish in abrasive-waterjet cutting. *Proc. 8th Int. Symposium on Jet Cutting Technology*, Durham, 1986, Paper 31, p. 309-313.
- [12] Henning, A., Westkamper, E. (2007). Modelling of contour generation in abrasive waterjet cutting. *Proc. 15th Int. Conf. on Jetting Technology*, Ronneby, p. 309-320.
- [13] Laurinat, A., Louis, H., Meier-Wiechert, G. (1993). A model for milling with abrasive water jets. *Proc. 7th American Water Jet Conf.* Seattle, Paper 8, p. 119-139.
- [14] Momber, A.W. (1995). A generalized abrasive water jet model. *Proc. 8th American Water Jet Conf.* Houston, Paper 25, p. 359-376.
- [15] Hashish, M. (1991). Optimization factors in abrasive-waterjet machining. *Trans. ASME, Journal of Engineering for Industry*, vol. 113, no.1, p. 29-37.
- [16] Zeng, J., Kim, T.J. (1993). Parameter prediction and cost analysis in abrasive waterjet cutting operations. *Proc. 7th American Water Jet Conf.* Seattle, Paper 11, p. 175-189.
- [17] Yong, Z., Kovacevic, R. (1997). 3D simulation of macro and micro characteristics for AWJ machining. *Proc. 9th American Water Jet Conf.*, Dearborn, Paper 9, p. 133-144.
- [18] Zhang, S., Shepherd, J.D., Summers, D.A. (2004). Experimental investigation of rectangular pocket milling with abrasive water jet using specially designed tool. *Proc. 17th International Conference on Water Jetting*, BHR Group, Mainz, p. 435-447.
- [19] Borkowski, P. (2004). Theoretical and experimental basis of hydro-jet surface treatment. *Publ. Koszalin University of Technology*, Koszalin, 328 p. (in Polish).
- [20] Borkowski, P., Zukocinski, T. (2006). Basis of three dimensional material forming using high-pressure abrasive-water jet controlled by virtual image luminance. *Advances in Manufacturing Science and Technology*, vol. 30, no. 1, p. 53-62.

- [21] Borkowski, P., Szpakowicz, A. (2008). Hydro-jetting shaping of bas-relief. *Journal of Machine Engineering*, vol. 13, no. 1-2, p. 81-89.
- [22] Borkowski, P. (2008). Creation of bas-relief basing on photography using high-pressure abrasive-water jet. *Journal of Machine Engineering*, vol. 8, no. 2, p. 43-51.
- [23] Borkowski, P., Szpakowicz, A. (2009). Abrasive-water jet shaping of bas-relief. *Proc. 2009 WJTA American Waterjet Conference*, Houston, Texas, Paper No. 3-A.
- [24] Borkowski, P., Zukocinski, T. (2006). Three dimensional method of material forming using high-pressure abrasive-water jet controlled by flat image luminance. *Proc. 18th Int. Conf. Jetting Technology*, Gdansk, p. 265-274.